First Principles Simulations of Silicon Nanoindentation

Rubén Pérez and Michael C. Payne
TCM, Cavendish Laboratory, University of Cambridge, Madingley Road, Cambridge CB3 OHE, United Kingdom

Alan D. Simpson
Edinburgh Parallel Computer Centre, University of Edinburgh, Mayfield Road, Edinburgh EH9 3JZ, United Kingdom
(Received 2 June 1995)

Total-Energy pseudopotential calculations are used to study the onset and development of plasticity in nanoindentation experiments. Plastic flow of atoms towards interstitial positions and extrusion of material towards the tip walls, stabilized by the adhesive interactions with the tip, are the dominant mechanisms. The delocalization of the charge induced by the stress in the elastically compressed structure triggers these plastic deformations. The onset of irreversible damage is related to the plastic deformation of the second double layer of the Si(111) surface.

PACS numbers: 62.20.Fe, 71.10.+x

The fabrication of structures where several of the characteristic dimensions approach the atomic limit has pervaded solid state physics for the past two decades. Characterization techniques have evolved in the same direction, probing the properties of matter on progressively shorter scales. This is the case of indentation experiments, where the use of an atomic force microscope with a sharp indenter has made it possible to reduce the depth of the indentation to just 1 nm [1]. Because of the high loads per atom reached in these nanoindentations, plasticity effects are expected to be particularly important.

Traditional theoretical approaches to the mechanical interaction between two materials brought into close contact, based on continuum elasticity and contact mechanics [2], are not suitable to describe this experimental regime. Atomic scale simulations provide a natural way to overcome the limitations of these models. Nanoindentation has been simulated for different systems using this approach: a metallic tip and a metal surface [3,4], and both a "smooth" tip and an "atomistic" tip indenting a silicon surface [5]. These studies have provided significant information about the process, but their results are limited by the use of simplified interatomic potentials, where the electronic degrees of freedom, crucial to describe the breaking and remaking of bonds involved in the plastic response, are not explicitly considered. The implementation of a standard total-energy pseudopotential method on a massively parallel computer [6] allows us to remove that limitation and to provide the first *ab initio* quantum mechanical simulation of the indentation process. The results of our study provide insight into the microscopic mechanisms involved in the onset and development of plasticity and the active role of the bonding sites of the tip in this process.

The system that we have considered is a supercell containing a hard metallic indenter, a Si(111) slab, and a vacuum region. The indenter is a sharp tetrahedral tip built up of twenty Al atoms stacked in four (111)-fcc planes. The relative positions of the atoms in the indenter are held fixed during the whole indentation process. This model retains the most important characteristics of a hard metallic tip, providing an accurate description of the bonding between the atoms in the surface and those on the tip, and allowing us to reach the highest possible stresses for a given indentation depth, and explore, with the limited computational resources available, the fundamental processes in the plastic deformation of the Si slab. The Si slab contains 240 atoms and is built up of eight (111) planes in an almost square two-dimensional $5 \times 3\sqrt{3}$ unit cell, each containing 30 atoms. The upper surface of the slab in contact with the tip has a 2×1 Pandey reconstruction [7]. The bottom surface is kept unreconstructed by saturating each dangling bond with an H atom. The total dimensions of the supercell,

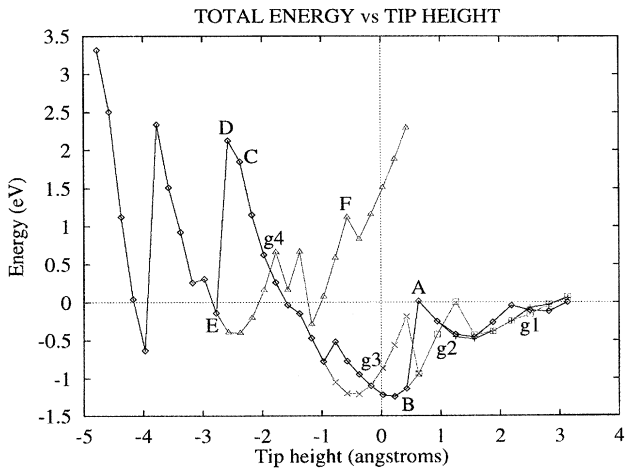

FIG. 1 (color). Total energy of the system as a function of the the tip height. The continuous black line corresponds to the indentation process while the different color lines (and symbols) refer to the retraction of the tip from different stages of the indentation process. The tip height is referred to the position of the last Si layer in an ideal Si(111) surface.

 0031-9007/95/75(26)/4748(4)$06.00

including the vacuum region of 6.26 Å, are 19.2 × 19.9 × 28.15 Å. Initially, the indenter is placed on top of the uppermost buckled atom in one of the π-bonded chains. The orientation of the tip is symmetric with respect to the (110) planes of the slab.

The indentation process was simulated in a stepwise, quasistatic manner by making small movements of the tip normal to the slab. At each step the atoms in the slab were allowed to relax to their equilibrium positions (zero forces) for that particular position of the tip [8]. Optimized nonlocal pseudopotentials [9,10] including only *s* and *p* components were used to describe the Al and Si ion cores [11]. The pseudopotentials were applied in the Kleinman-Bylander form [12], using the real space projection technique [13]. The electronic states were expanded at the Γ point of the Brillouin zone. A cutoff for the plane wave basis set of 7 Ry was used .

The total energy of the system for the different positions of the tip during the indentation process (black continuous line) and the retraction of the tip from different stages of the indentation (colored lines) is shown in Fig. 1. We'll consider first the indentation process. The results show a pattern of elastic deformations followed by plastic deformations seen as discontinuous jumps in the energy. These plastic deformations are associated with the breaking of a few bonds where the stress has accumulated during the elastic regime. A few atoms in the structure undergo large displacements (of the order of 1 Å) to form a new stable bonding configuration in which the stress has been released. This new structure is elastically deformed

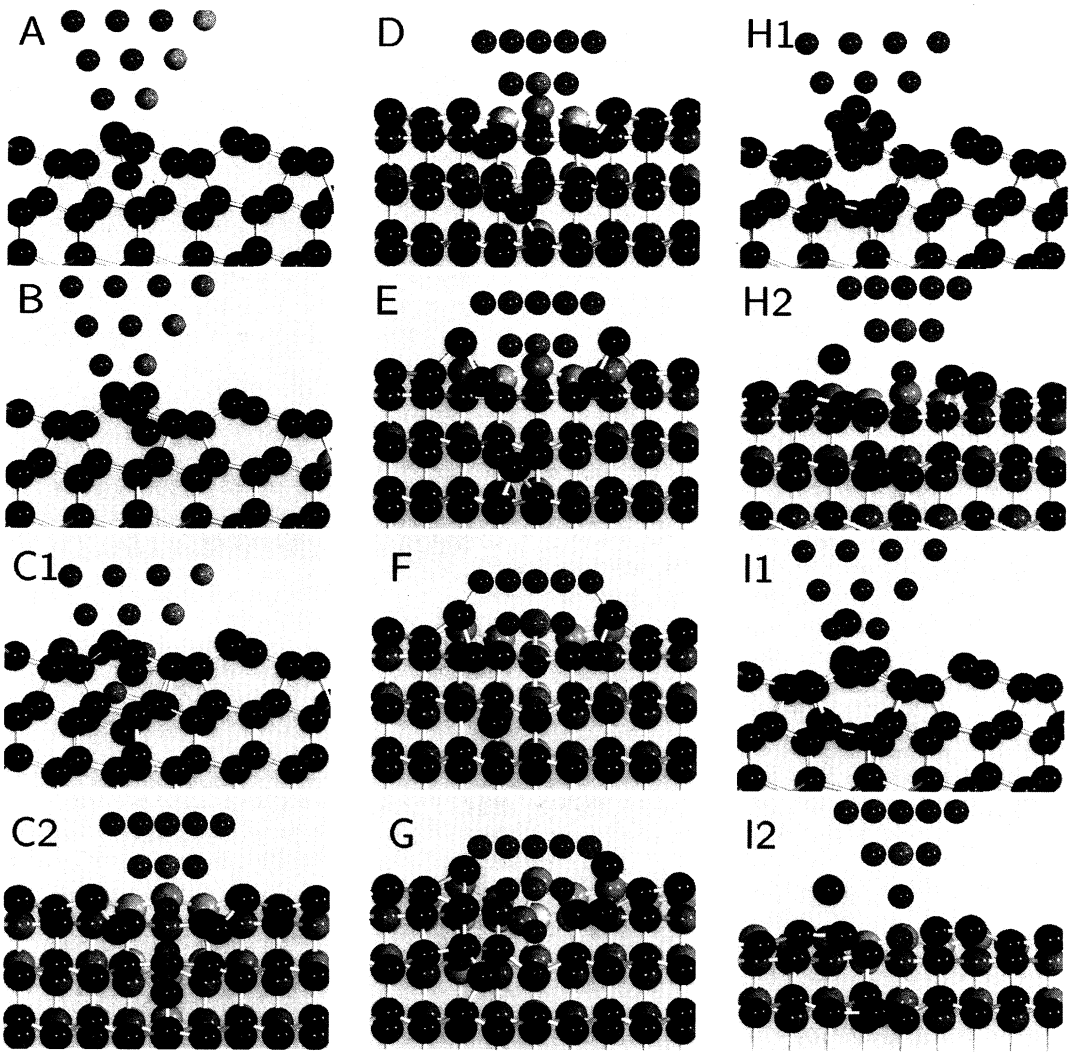

FIG. 2 (color). Ball-and-stick model of the atomic configurations for some of the steps labeled in Fig. 1 [(a)–(g), indentation process, and (h)–(i), retraction of the tip]. (a) and (b) correspond to frontal views of the system (along the [1$\bar{1}$0] direction), (d)–(g) to lateral views (along the [11$\bar{2}$] direction), while frontal and lateral views are shown for (c), (h), and (i). In the lateral view, part of the atoms have been removed to appreciate the displacements of the atoms below the tip in the center of the slab.

upon further loading. The other remarkable feature in the total-energy curve is that it shows work hardening of the material: The stress necessary to produce those plastic deformations increases with the deformation. It should be noticed that this is an intrinsic process, different from the usual strain hardening associated with the pinning of dislocations.

We now analyze the atomistic processes involved in plastic flow for the different stages of the indentation process. Figure 2 shows a ball-and-stick model of the atomic configurations for the different steps labeled in Fig. 1. Figure 2(a) represents the structure of the system before the first discontinuous jump. The Si atom which was just below the tip has bonded to the apex atom in the first stages of the indentation. Since then it has been moving down, breaking the bonds with the atoms in the chain and making new bonds with the atoms below. During the jump, this atom moves more than 1 Å in the direction perpendicular to the chains, across the interstitial (Fig. 2(b)). These plastic deformations are triggered by the delocalization of the charge density induced by the stress in the elastically compressed structure, as seen in Fig. 3 [14].

During the following steps, two different processes are taking place at the surface and inside the slab. At the surface, an increasing number of atoms in the first Si double layer are coordinated with atoms in the walls of the tip. The competition between the bonds formed with the atoms in the tip and the elastic deformation induced in the Si tetrahedral network determines that, upon further indentation, those atoms undergo a stick-slip motion along the walls of the tip, recovering positions in the direction of indentation which are very close to the ones in the original undeformed structure. This stick-slip motion is responsible for the friction, and hence the dissipation observed in earlier simulations [5]. Inside the slab, the atom originally below the tip tries to make its way below the second double layer, following a path of high coordination through one of the sides of a tetrahedra in the second double layer, pushing the central atom and breaking its bond with the two other neighbors in the double layer [see Fig. 2(c)]. The remarkable feature of all of these processes is that the induced deformation pattern is symmetric with respect to the (110) plane passing through the apex of the tip, with the plastic displacement of atoms below the tip confined to (110) planes, as can be seen in Fig. 2(c).

After this step the system can no longer resist the induced stress with a pure elastic deformation, and plastic flow in the second double layer is induced. The transition to this new regime is mediated by the *spontaneous* breaking of the symmetry of the displacement pattern in the [110] direction. The main atomistic process involved is the displacement of the atom by more than 1 Å in the [110] direction towards the interstitial, the direction of the Burgers vector for screw dislocations in the (111) slip system [see Fig. 2(d)]. This process is completed during the jump,

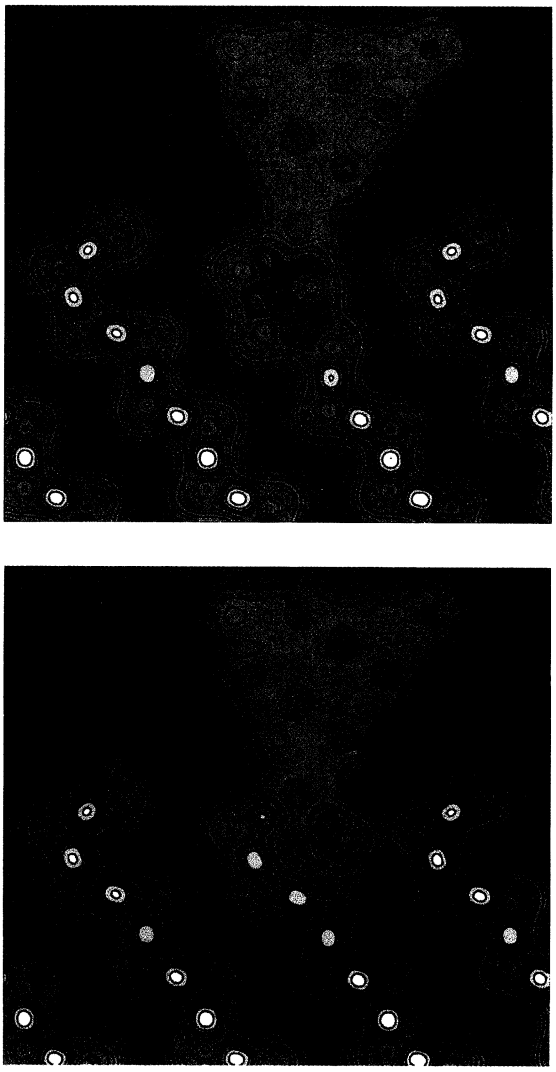

FIG. 3 (color). Charge densities in a (110) plane going through the middle of the tip for the steps labeled A (above) and B (below) in Fig. 1. The higher densities (above 0.55 eV/Å^3) correspond to yellow and the lowest ones (below 0.05 eV/Å^3) to dark blue. The spacing between two consecutive contours corresponds to 0.05 eV/Å^3.

with this atom moving to a stable position in the interstitial; the atom which was below the tip moving down (0.76 Å) below the second double layer to another interstitial position in a parallel (110) channel, and a general recovery of the elastic displacements in the structure [Fig. 2(e)]. During that jump, another process takes place at the surface of the sample which contributes to release the stress in the structure: the extrusion of material (with atoms moving more than 1 Å up) towards the walls of the tip [Fig. 2(e)]. This deformation is induced by the nonuniform volume strain created in the indented area and stabilized by the adhesive interactions with the tip [14]. These two mechanisms, the plastic flow to the interstitials and the shear flow

around the indenter, dominate the plastic response in this regime. As indentation proceeds the plastically deformed areas in the surface and below the indenter make contact, and we reach the full plastic flow regime, with plastic deformation inside the slab becoming easier because of the upward displacements of atoms in the planes above [see Figs. 2(f) and 2(g)] [14]. The evolution of plastic flow observed in the simulation supports the model used in some continuum elastic theories of the indentation contact to include plasticity effects [15].

As mentioned before, we have also performed simulations pulling the tip back from different stages of the indentation process. The total energy for the different steps in these simulations (colored lines in Fig. 1) shows hysteresis, with several different stable structures for a given value of the tip height, and the system following different paths in the different backward displacements. This hysteric behavior is related to the breaking of the bonds already formed between the tip and the sample during the loading process. More importantly, the plot shows a transition from perfect recovery of the original structure of the Si slab for small indentations to permanent damage when we unload from a point beyond the step where the symmetry has been broken in the forward displacement. Although the configuration obtained for the last steps in that simulation [see Figs. 2(h) and 2(i)] shows an important elastic recovery, the residual stresses are unable to reverse some of the plastic strains below the tip, and several atoms remain in interstitial positions. The damage is not confined to the bulk of the slab, and changes in the bonding topology of the surface can be seen in Figs. 2(h) and 2(i), where one of the Si atoms is moving apart with the tip. These results relate the onset of permanent damage in the material to plastic deformations in the second double layer.

Finite temperature and strain rate effects not considered in our quasistatic $T = 0$ simulations are known to influence the indentation process. An estimate of their effect can be obtained by calculating the energy barriers at the crossing points between the different stable structures found in the total-energy diagram. These barriers have been determined for four different crossings (labeled k1–k4 in Fig. 1). In the first three cases (k1–k3), the barriers are quite low: 0.10, 0.12, and 0.30 eV. These processes can easily be thermally activated, and the system would follow the lowest energy structure available, avoiding states of high stress such as A. On the contrary, the last transformation (k4) has a high barrier of 1.2 eV. A more detailed account of the influence of temperature and strain rate will be given elsewhere [14].

In conclusion, we have presented the first quantum mechanical simulation of a nanoindentation process. The atomic mechanisms for plastic deformation in this regime have been determined: plastic flow of atoms towards interstitial positions inside the slab, and extrusion of material towards the tip at the surface, induced by the nonuniform volume strain and stabilized by the adhesive interactions with the tip. These adhesive interactions, disregarded in many continuum approaches to the problem, are also shown to be responsible for the friction through the induced stick-slip motion of Si atoms along the walls of the tip, the hysteric behavior observed in the simulations pulling the tip out from different stages of the indentation process, and the recovery of plastic strains during unloading. Finally, the onset of plastic irreversible deformation of the sample is related to the plastic deformation of the second double layer of the slab.

The highly symmetric position and sharp indenter considered in this work have allowed us to explore the fundamental processes in the plastic limit. Further insight into the details of the nanoindentation process could be gained considering simulations with different structures for the tip and different initial positions on the surface.

These calculations were performed as a part of the "Grand Challenge" collaborative project, coordinated by Professor M. J. Gillan, on the Cray T3D at the Edinburgh Parallel Computing Centre. R. P. acknowledges the financial support of the Human Capital and Mobility Programme of the European Union under Contract No. ERBCHBICT93-0779. We thank Dr. C. Molteni and Professor V. Heine for useful conversations.

[1] B. Bhushan and V. N. Koinkar, Appl. Phys. Lett. **64**, 1653 (1994).
[2] K. L. Johnson, *Contact Mechanics* (Cambridge University Press, Cambridge, 1985).
[3] J. B. Pethica and A. P. Sutton, J. Vac. Sci. Technol. A **6**, 2494 (1988); A. P. Sutton *et al.*, in *Electron Theory in Alloy Design*, edited by D. G. Pettifor and A. H. Cottrell (The Institute of Materials, London, 1992), pp. 191–233.
[4] U. Landman, W. D. Luedtke, N. A. Burnham, and R. J. Colton, Science **248**, 454 (1990); U. Landman *et al.*, in *Scanning Tunneling Microscopy III*, edited by R. Wiesendanger and H.-J. Güntherodt (Springer, Berlin, 1993), pp. 207–259.
[5] J. S. Kallman *et al.*, Phys. Rev. B **47**, 7705 (1993).
[6] M. C. Payne *et al.*, Rev. Mod. Phys. **64**, 1045 (1992).
[7] K. C. Pandey, Phys. Rev. Lett. **60**, 2156 (1988); F. Ancilotto *et al.*, *ibid.* **65**, 3148 (1990).
[8] The total energy was converged to within less than three-thousands of eV per supercell and the forces in the atoms to less than 0.03 eV/Å at each step.
[9] A. Rappe *et al.*, Phys. Rev. B **41**, 1227 (1990).
[10] J. S. Lin *et al.*, Phys. Rev. B **47**, 4174 (1993).
[11] The core radii used to generate the pseudopotentials are 1 Å for Si and 1.26 Å for Al. During our simulations, the minimum distance between the atoms, even in the highly compressed stages of the simulation, remains large enough for the cores not to overlap.
[12] L. Kleinman and D. M. Bylander, Phys. Rev. Lett. **48**, 1425 (1982).
[13] R. D. King-Smith, M. C. Payne, and J-S. Li, Phys. Rev. B **44**, 13 063 (1991).
[14] R. Perez and M. C. Payne (to be published).
[15] J. S. Field and M. V. Swain, J. Mater. Res. **8**, 297 (1993).

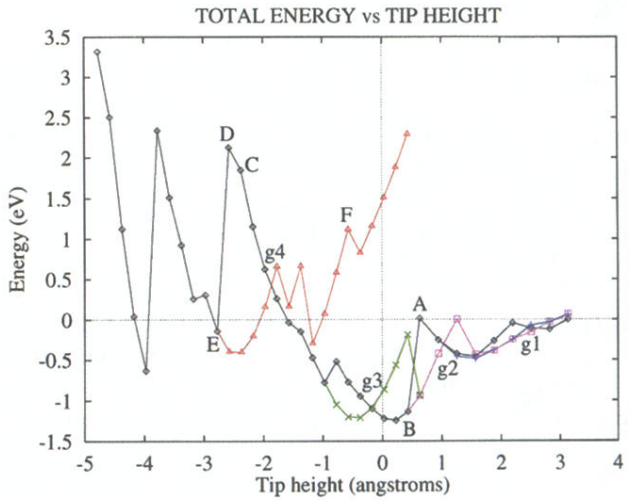

FIG. 1 (color). Total energy of the system as a function of the the tip height. The continuous black line corresponds to the indentation process while the different color lines (and symbols) refer to the retraction of the tip from different stages of the indentation process. The tip height is referred to the position of the last Si layer in an ideal Si(111) surface.

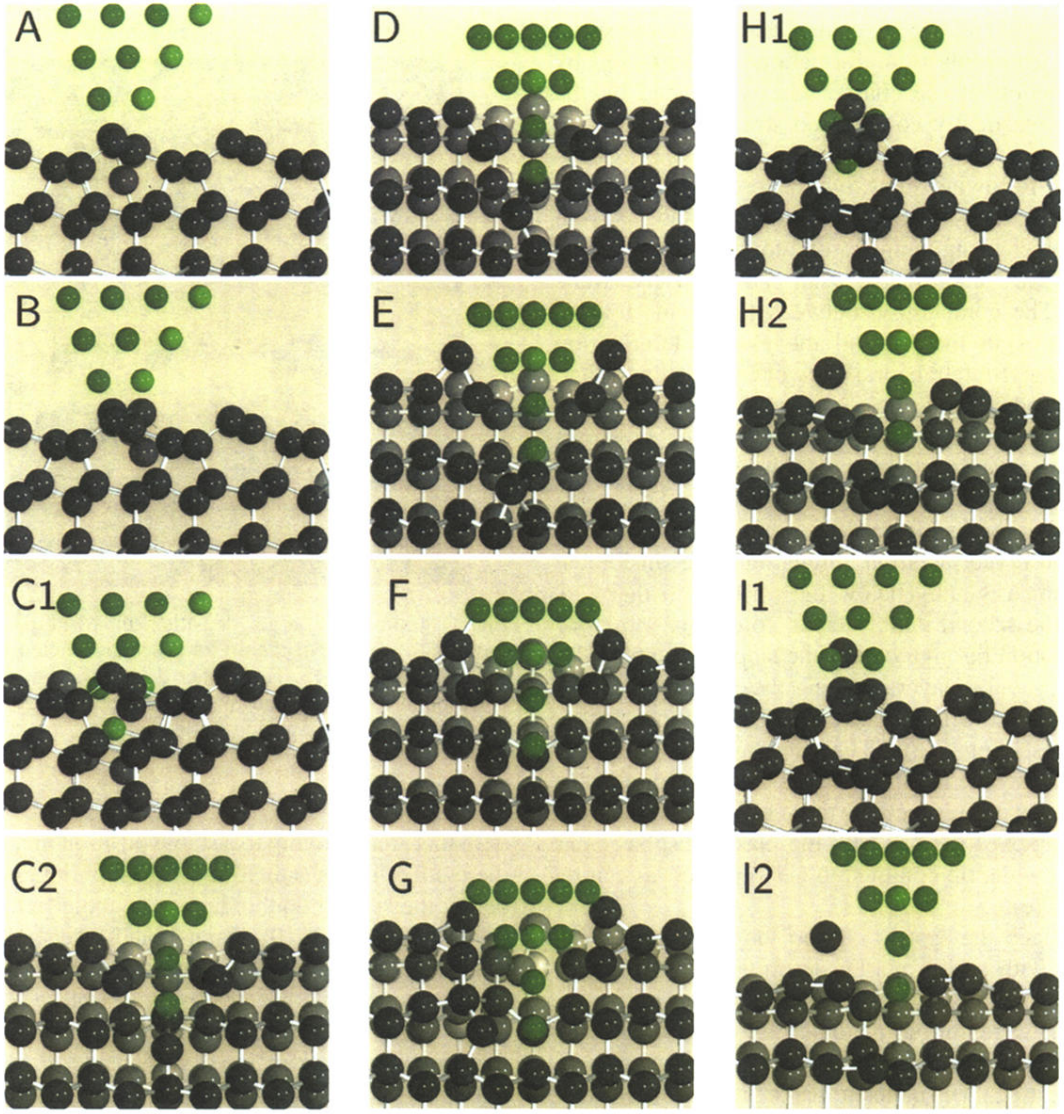

FIG. 2 (color). Ball-and-stick model of the atomic configurations for some of the steps labeled in Fig. 1 [(a)–(g), indentation process, and (h)–(i), retraction of the tip]. (a) and (b) correspond to frontal views of the system (along the $[1\bar{1}0]$ direction), (d)–(g) to lateral views (along the $[11\bar{2}]$ direction), while frontal and lateral views are shown for (c), (h), and (i). In the lateral view, part of the atoms have been removed to appreciate the displacements of the atoms below the tip in the center of the slab.

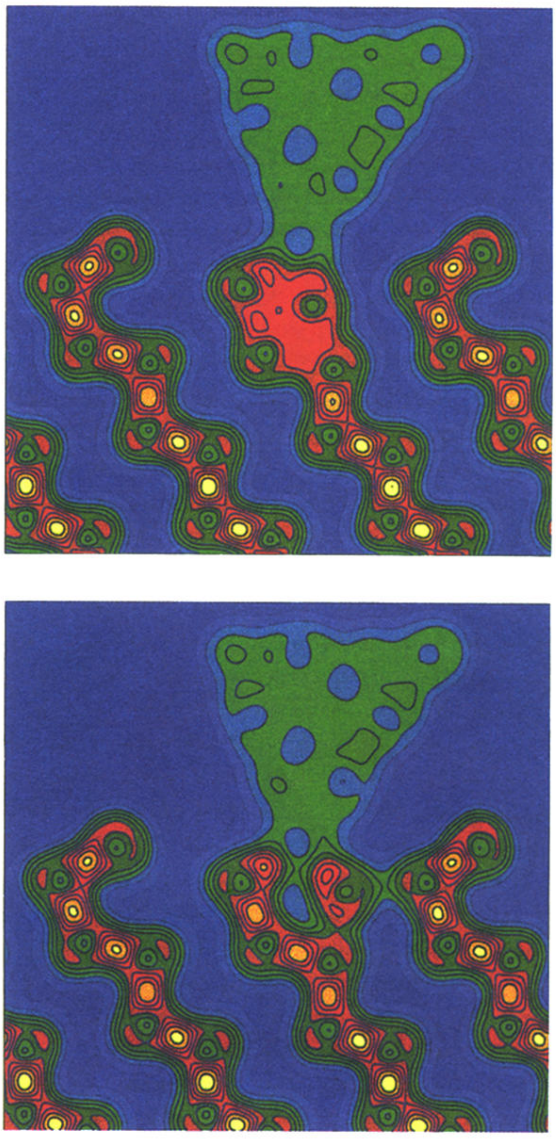

FIG. 3 (color). Charge densities in a (110) plane going through the middle of the tip for the steps labeled A (above) and B (below) in Fig. 1. The higher densities (above 0.55 eV/Å^3) correspond to yellow and the lowest ones (below 0.05 eV/Å^3) to dark blue. The spacing between two consecutive contours corresponds to 0.05 eV/Å^3.